SAND2015-11108C

MINIMAL VARIATION OF DEFECT STRUCTURE DUE TO THE ORDER OF ROOM TEMPERATURE HYDROGEN ISOTOPE IMPLANTATION AND SELF-ION IRRADIATION IN NICKEL

Brittany Muntifering[1,2], Jianmin Qu[2,3], Khalid Hattar[1]

[1]Sandia National Laboratories, Albuquerque, NM, 87185, U.S.A.
[2]Northwestern University, Evanston, IL, 60208, U.S.A.
[3]Tufts University, Medford, MA, 02155, U.S.A.

ABSTRACT

The formation and stability of radiation-induced defects in structural materials in reactor environments significantly effects their integrity and performance. Hydrogen, which may be present in significant quantities in future reactors, may play an important role in defect evolution. To characterize the effect of hydrogen on cascade damage evolution, in-situ TEM self-ion irradiation and deuterium implantation was performed, both sequentially and concurrently, on nickel. This paper presents preliminary results characterizing defect formation and evolution during room temperature deuterium implantation and self-ion irradiation and the consequence of the sequence of irradiation. Hydrogen isotope implantation at room temperature appears to have little or no effect on the final defect structures that result from self-ion irradiation, regardless of the sequence of irradiation. Tilting experiments emphasize the importance of precise two-beam conditions for characterizing defect size and structure.

INTRODUCTION

The structural materials used in fusion reactors will be exposed to high energy neutrons that result in atomic displacement cascades and transmutation reactions, which produce significant quantities of helium and hydrogen isotopes. Plasma facing materials are also exposed to high flux, low energy plasma ions including helium and hydrogen isotopes. It is generally assumed that hydrogen is not trapped very effectively at room temperature in most metals due to its high mobility and solubility [1]; however, radiation induced damage in the form of vacancies and vacancy clusters may act as hydrogen traps. Recent experimental results suggest that, in certain temperature ranges, there may be a synergistic effect of hydrogen with displacement damage and helium, which results in an increase in swelling and material hardening in comparison to displacement damage and helium alone [2]. To assist in the selection of structural materials for future nuclear reactors, and as a guide to new material development, it is critical to develop an understanding of the mechanisms involved in hydrogen enhanced materials degradation. In this study, in-situ transmission electron microscopy (TEM) self-ion irradiation and deuterium implantation was performed, both sequentially and concurrently, at room temperature on nickel. Nickel was chosen as a model face-centered cubic system to gain insight into mechanisms involved in the hydrogen-displacement cascade interplay for more complicated austenitic steels. These preliminary results suggest that hydrogen isotope implantation at room temperature has little or no effect on the final defect structures that result from self-ion irradiation, regardless of the sequence of irradiation.

EXPERIMENTAL PROCEDURE

To elucidate mechanisms involved in irradiation defect evolution and the associated effects of hydrogen isotopes, coarse grained nickel [3], which had been electropolished in a solution of 20% Perchloric Acid/80% Acetic Acid at 0˚C, was irradiated with D_2^+ and Ni^{3+} ions, both sequentially and concurrently, in the TEM. In-situ ion irradiation TEM experiments were conducted at room temperature in a JEOL 2100 TEM operated at 200 kV [4]. A 6 MV High Voltage Engineering (HVE) Tandem accelerator was used to generate and accelerate a 3 MeV Ni^{3+} beam and a 10 kV Colutron ion accelerator was used to accelerate a 10 kV D_2^+ beam. The two ion beams entered the TEM along nominally the same path, nearly orthogonal to the electron beam. The nickel TEM samples were tilted approximately 30˚ towards the ion beams and video recordings at a rate of 15 frames per second provided real time nanoscale observations during implantation and irradiation. To investigate the consequence of the sequence of irradiation, three separate experiments were performed. In the first experiment, the nickel sample was first implanted with 10 kV D_2^+ ions at an average flux of 2.5 x 10^{14} D_2^+/cm^2s to a total fluence of 2.3 x 10^{17} D_2^+/cm^2, resulting in approximately 2 displacements per atom (dpa). All damage estimates are predicted by SRIM simulation performed under "detailed calculation with full damage cascade" mode [5]. The sample was then irradiated with 3 MeV Ni^{3+} ions at an average flux of 4×10^{11} Ni^{3+}/cm^2s and an average displacement rate of 1.3 x 10^{-3} dpa/s to an approximate total fluence of 6.2 x 10^{14} Ni^{3+}/cm^2 and an average of 2 dpa, resulting in 4 dpa total. The second sample was subjected to the reverse order of irradiation, such that it was first self-ion irradiated and then deuterium implanted to the same total fluence and damage levels as the first experiment. For the third sample, the deuterium flux was decreased to 1.5 x 10^{14} D_2^+/cm^2s. The sample was then irradiated with D_2^+ and Ni^{3+} concurrently to the same total fluence and damage level (4 dpa) as the previous experiments.

SRIM simulations [5] suggested that 3 MeV nickel ions would pass fully through the film and create a nearly uniform damage profile. The damage profile from deuterium is not uniform; instead, the damage is heavily concentrated at the entrance side of the film and drops rapidly throughout the film. The deuterium ions are expected to reach a maximum concentration approximately 40 nm from the entrance surface of the film and a maximum depth of approximately 100 nm. ImageJ software was used to measure the diameter of visible dislocation loops in the bright field images.

RESULTS AND DISCUSSION

The first part of this study involved room temperature self-ion irradiation and deuterium implantation, in both forward and reverse order, to study the effect of the sequence of ion irradiation on the final defect microstructure. The self-ion irradiation and deuterium implantation is then performed concurrently and compared to sequential results.

In the first experiment, a nickel sample was implanted with deuterium to a final dose of 2.3 x 10^{17} D_2^+/cm^2, which resulted in approximately 2 dpa. After implantation, a low density of nanometer sized defects was visible. Previous work by other groups involving deuterium implantation in nickel has shown that these defects are interstitial dislocation loops [6-8], likely resulting from single interstitial atoms created during deuterium irradiation slowly accumulating into visible defects. The nickel sample was then immediately self-ion irradiated to a total dose of

6.2 x 10^{14} Ni^{3+}/cm^2, resulting in an additional 2 dpa. The combined ion irradiation resulted in a total of 4 dpa. Figure 1a and b are bright field and weak beam images (**g** = 600), which show the defect microstructure after deuterium implantation and self-ion irradiation. Significant radiation damage is visible in the form of black spots in bright field (Figure 1a) and white spots in weak beam images (Figure 1b), which are presumed to be small dislocation loops. Figure 1c is a histogram of the size distribution of visible loops, measured in the bright field image.

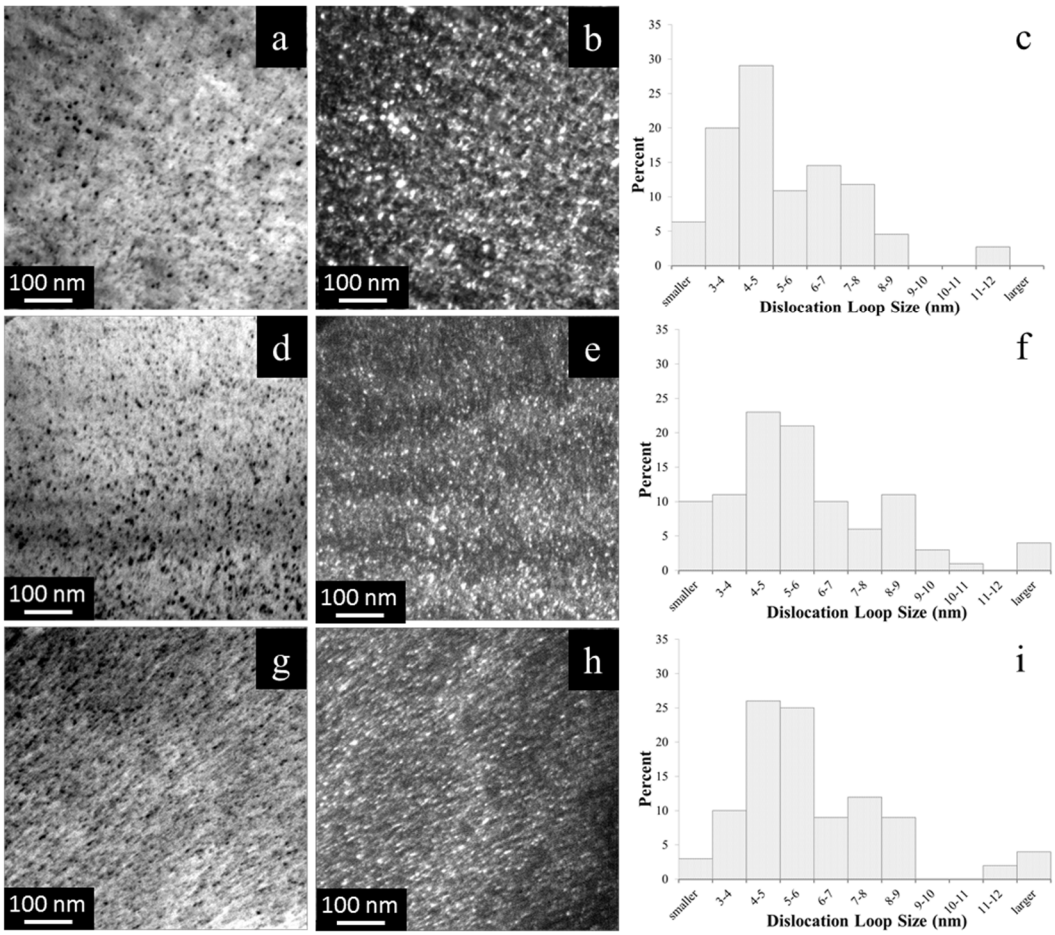

Figure 1 Bright field and weak beam images (**g** = 600), and corresponding histograms of dislocation loop sizes for a-c) Nickel sample which is first implanted with deuterium and then self-ion irradiated d-f) sample which was first self-ion irradiated then deuterium implanted g-i) Nickel sample which was concurrently self-ion irradiated and deuterium implanted. Nanometer sized damage clusters are visible as black spots in bright field images (a,d,g) and white spots in weak beam images (b,e,h).

The second experiment involved the reverse order of irradiation, in which the sample was first self-ion irradiated and then deuterium implanted for a total of 4 dpa, and the resulting microstructure is shown in Figure 1d-e and the corresponding size distribution is shown in Figure 1f. Video recordings during self-ion irradiation show dislocation loops appearing in a single frame, consistent with cascade collapse. This is demonstrated in Figure 2, where Figure 2a and b are weak beam images taken from video recordings and are sequential frames (1/15 s). Figure 2c is a difference image of Figures 2 a and b, the image contrast is the result of the rapid appearance

of a dislocation loop in the center of the frame. Very few loops were seen to escape through the surface of the film, and only a small fraction of loops were mobile and seen to glide small distances in one-dimension on the order of several nanometers. The majority of the loops were stable at this temperature. No signs of hydrogen enhanced localized plasticity [9] was seen to result from the introduction of deuterium from ion implantation. This result may be due to the role of vacancies that are simultaneously predicted to be introduced into the sample during the deuterium implantation and may subsequently serve as trapping sites.

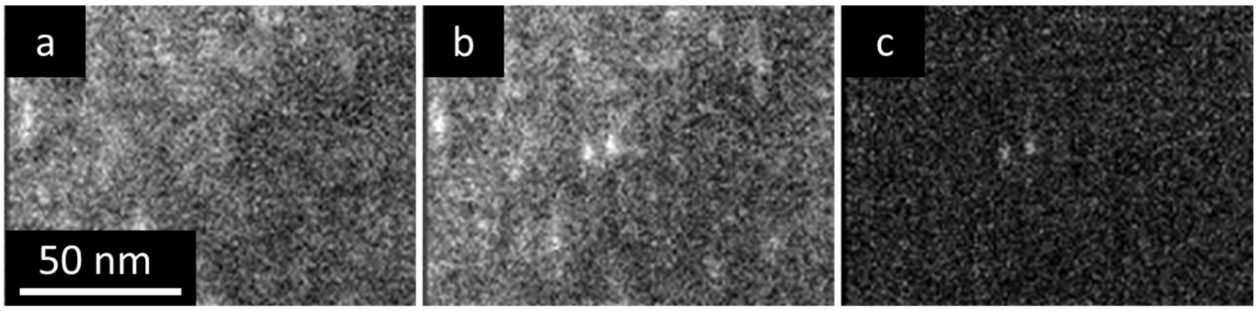

Figure 2 a-b) Sequential frames from video recordings during self-ion irradiation c) difference image between Figure 2 a and b showin the appearance of a dislocation loop. This is consistant with cascade damage in nickel caused by self-ion irradiation.

Figure 1 g-h show the results of the third experiment, in which the sample is concurrently deuterium implanted and self-ion irradiated, and Figure 1i shows the size distribution of the dislocation loops. All sequences of irradiation and hydrogen isotope implantation resulted in a large density of nanometer sized dislocation loops; however, through-focus imaging did not reveal visible cavities in any case. Irradiation induced vacancies and vacancy clusters are immobile in nickel at room temperature. It has been shown that these vacancy clusters are strong traps for deuterium [10-12], such that cavities may eventually be expected to form during deuterium implantation. Other groups have observed that deuterium implantation in nickel created large cubic cavities on the order of tens of nanometers wide, but only in a narrow temperature range around 300 to 400 ºC and only near dislocations and dislocation loops [6-8,13]. These experiments suggest that the next step in characterizing the significance of the sequence of implantation and irradiation will require repeating this set of experiments at elevated temperatures and characterizing the effect of irradiation sequence on cavity formation.

ImageJ was used to measure the size of loops in bright field images in Figure 1a,d,g, which were each taken close to $\mathbf{g} = 600$. In each case, a monomodal distribution centred around 5 nm was present, with an average of 5.5 ± 1 nm and no significant statistical difference in size distribution was present, as seen in figures 1c,f,i. Previous experiments have suggested that the implanted hydrogen isotope atoms enhance loop formation and hydrogen-vacancy complexes may act as nucleation sites for loops [8,13]. However, at room temperature the loops created during cascade collapse caused by self-ion irradiation appear to be stable (Figure 2). It is likely that in this temperature range the deuterium-vacancy complexes do not interact with stable dislocation loops. Implantation at higher temperatures, where loops may be more mobile, may shed more light on the role that Deuterium-Vacancy complexes play in defect evolution, in addition to the study of cavity formation discussed earlier.

Figure 3 is a series of images of the sample which was first deuterium implanted then self-ion irradiated. The left grain in Figure 3a is oriented approximately 5º from the [011] zone axis in a two beam condition with **g** = 200 (diffraction pattern inset). The burgers vector of the dislocation loops is likely ½ <110>, and the loops should be visible in this imaging condition. Instead, the contrast in the left grain is dominated by oxide and bending, such that the dislocation loops are not easily distinguished. In Figure 3b, the sample has been tilted 0.4º from Figure 3a, such that **g** = 400. In this case the dislocation loops have enough contrast to be easily distinguished. The loop density was measured to be 4.3 x 10^{11} defects/cm^2 and average loop size was 6.3 nm. Figure 3c has been titled an addition 0.4º so that **g** = 600. In this case, the loops are easy to distinguish and appear smaller than those in Figure 3b, with a measured density of 6.0 x 10^{11} defects/cm^2 and an average size of 5.0 nm. Figure 3d is tilted another 0.4º (for a total of 1.2º tilt from figure 3a) to **g** = 800. The loops are easy to distinguish, and loops that appeared as one large loop in Figure 3b are easy to distinguish as separate small loops. In this case, the measured loop density was 9.3 x 10^{11} defects/cm^2 with an average size of 4.5 nm. The grain on the right side is also now in a diffracting condition in which the loops can be distinguished. The series of images in Figure 3 demonstrate why it is challenging to quantitatively compare TEM images of loops from different samples or even different areas of the same sample. For example, irradiation and the associated heating effects often cause sample bending of several degrees, and care must be taken when analysing video recordings of defect evolution during irradiation as the sample may likely bend during the video. Figure 3 also demonstrates the difficulty in comparing images from different samples, such as in Figure 1. All images in Figure 1 were taken close to **g** = 600 conditions; however, significant local bending is apparent in the samples, as dislocation loop size appears to vary and contrast changes inside each image.

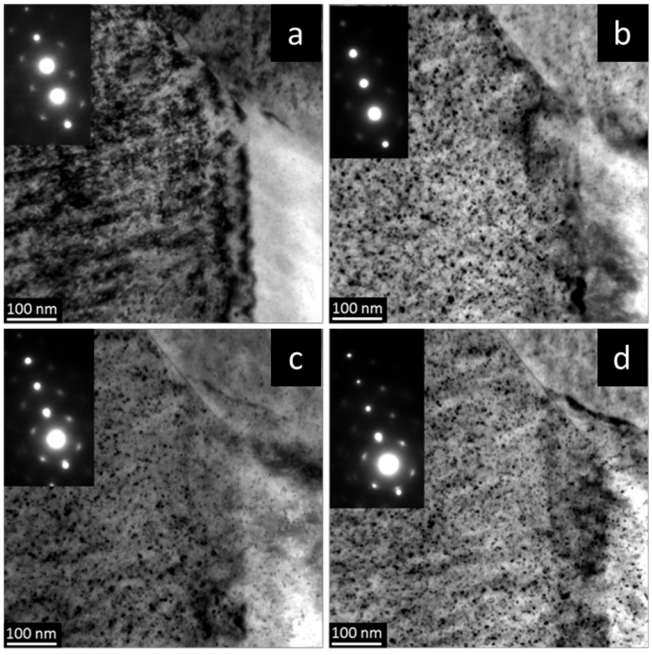

Figure 3 Bright field TEM images of nickel sample which was implanted with deuterium and then self-ion irradiated. a) Grain on the left side of images is in a two beam condition with **g** = 200. High contrast makes dislocation loops indiscernible. b) Sample tilted 0.4º to **g** = 400 in which dislocation loop contrast is increased enough to be discernable. c) Sample tilted additional 0.4º to **g** = 600 and d) **g** = 800, in this condition small loops are easy to distinguish.

CONCLUSIONS

Deuterium implantation and self-ion irradiation, in both sequences as well as concurrently, were performed in-situ in the TEM on nickel samples at room temperature. Dislocation loops formed in all conditions with similar size distributions in all cases and no cavities were visible in any case. Dislocation loops caused by self-ion irradiation at this temperature were seen to be stable and with low mobility, such that deuterium did not play a significant role in the final defect density and size. Tilting experiments to different **g** conditions demonstrate the challenge in characterizing defect size and density and comparison between samples. Future experiments will involve elevated temperature irradiation and implantation, in both sequences and concurrently, to characterize the effect of sequence on cavity formation.

ACKNOWLEDGMENTS

The authors would like to thank D. Buller and D. Bufford for their experimental assistance and useful conversation, as well as S. Lawrence, D. Medlin, and M. Homer for providing the material. This work is primarily supported by the US Department of Energy's Nuclear Energy University Program (DE-NE0000678). Sandia National Laboratories is a multi-program laboratory managed and operated by Sandia Corporation, a wholly owned subsidiary of Lockheed Martin Corporation, for the U.S. Department of Energy's National Nuclear Security Administration under contract DE-AC04-94AL85000.

REFERENCES

[1] Lewis, F. A., *Pure and Applied Chemistry* 62.11 (1990): 2091-2096.
[2] Marian, Jaime, et al., *Journal of Nuclear Materials* (2014).
[3] Lawrence, Samantha K., et al., *JOM* 66.8 (2014): 1383-1389.
[4] K. Hattar, D. C. Bufford, and D. L. Buller, *Nuclear Instruments & Methods in Physics Research Section B,* vol. 338, pp. 56-65, Nov 1 2014.
[5] J. F. Ziegler, M. D. Ziegler, and J. P. Biersack, *Nuclear Instruments & Methods in Physics Research Section B-Beam Interactions with Materials and Atoms,* vol. 268, pp. 1818-1823, 2010.
[6] K. Niwase, T. Ezawa, T. Tanabe, and F. E. Fujita, *Journal of Nuclear Materials,* vol. 160, pp. 229-241, Dec 1988.
[7] K. Niwase, T. Ezawa, T. Tanabe, M. Kiritani, and F. E. Fujita, *Journal of Nuclear Materials,* vol. 203, pp. 56-66, Jul 1993.
[8] K. Ono, R. Sakamoto, T. Muroga, and N. Yoshida, *Journal of Nuclear Materials,* vol. 233, pp. 1040-1044, Oct 1996.
[9] Robertson, I. M., *Engineering Fracture Mechanics* 68.6 (2001): 671-692.
[10] G. A. Raspopova and V. L. Arbuzov, *Physics of Metals and Metallography,* vol. 107, pp. 58-67, Jan 2009.
[11] I. Takagi, K. Yoshida, K. Shin, and K. Higashi, *Nuclear Instruments & Methods in Physics Research Section B-Beam Interactions with Materials and Atoms,* vol. 84, pp. 393-399, 1994.
[12] V. L. Arbuzov, G. A. Raspopova, S. E. Danilov, A. P. Druzhkov, and Y. N. Zouev, *Journal of Nuclear Materials,* vol. 283, pp. 849-853, Dec 2000.
[13] N. Yoshida, M. Yasukawa, and T. Muroga, *Journal of Nuclear Materials,* vol. 205, pp. 385-393, Oct 1993.